Hindawi
Geofluids
Volume 2021, Article ID 5583191, 22 pages
https://doi.org/10.1155/2021/5583191

Research Article

The Lithological Features of Sublacustrine Fans and Significance to Hydrocarbon Exploration: A Case Study of the Chang 7 Interval of the Yanchang Formation, Southeastern Ordos Basin, North China

Bo Yang[1], **Hongjun Qu**[1], **Jianchao Shi**[2,3], **Yuqi Bai**[2,3], **Wenhou Li**[1], **Yanrong Zheng**[1], **and Rongjun Zhang**[4]

[1]*State Key Laboratory of Continental Dynamics, Department of Geology, Northwest University, Xi'an, Shaanxi 710069, China*
[2]*National Engineering Laboratory of Low-Permeability Oil & Gas Exploration and Development, Xi'an, Shaanxi 710018, China*
[3]*Exploration and Development Research Institute, PetroChina Changqing Oilfield Company, Xi'an, Shaanxi 710018, China*
[4]*Shaanxi Key Laboratory of Advanced Stimulation Technology for Oil & Gas Reservoirs, College of Petroleum Engineering, Xi'an Shiyou University, Xi'an 710021, China*

Correspondence should be addressed to Bo Yang; yangb_nwu@163.com and Hongjun Qu; 276299617@qq.com

Received 23 January 2021; Revised 23 February 2021; Accepted 18 March 2021; Published 8 May 2021

Academic Editor: Zhigang Tao

The Chang 7 interval of the Upper Triassic Yanchang Formation in the Ordos Basin represents a typical deep lacustrine depositional sequence. On the basis of field outcrops, cores, well logs, light/heavy mineral provenance analysis, and petrological studies, we evaluated the characteristics of deep-water gravity flow deposition of the Chang 7 interval and constructed a depositional model. The sediments mainly came from the northeast of the study area, and multiple sublacustrine fans were deposited in the center of the basin. Different from the deep-marine fan, the sublacustrine fan in the study area develops under the background of gentle slope without any erosional canyon between the fan and delta front. Gravity flow deposits in the study area can categorised into three groups: sand debris flow deposits, turbidity current deposits, and deep-water mudstone deposits. The main channel and branch channel are mainly developed with thick massive sandy debris sandstone, while the channel lateral margin and branch channel lateral margin are mainly developed with middle massive sandy debris sandstones and turbidite sandstones, which from bottom to top, the thickness of sand layer becomes thinner and the grain size becomes smaller. Thin mudstone is developed between channels; the lobe fringe includes sheet-like turbidite sandstones and deep lake mudstones. The widely distribute, good quality source rocks (TOC = 2% – 6%) developed in deep lacustrine have attained the peak stage of oil generation (R_o = 0.9% – 1.2%). The superimposition of the sublacustrine fan sand bodies and the wide distribution of good quality source rocks favor the formation of large lithologic reservoirs characterized by source–reservoir integration, self-generation and self-storage, and near-source accumulation.

1. Introduction

The continuous development of new technology and advances in knowledge on oil and gas exploration and development have remarkably improved exploration and development in deep-water basins worldwide. Major discoveries of oil and gas in tight sandstones include the Gulf of Mexico, the North Sea, and the Norwegian Sea [1–10]. These discoveries prompted deep-water exploration in marine basins such as the Qiongdongnan and the Yinggehai and continental basins such as the Ordos and the Bohai Bay in China. Concurrently, theoretical advancements improved understanding of deep-water sedimentation [11, 12]. Deep-water gravity flows sedimentary models were primarily developed between 1950 and 1970, such as the Bouma sequence, the York model, and the ancient submarine fan model [13–18].

As understanding of deep-water sediments improved, Shanmugam proposed a deep-water model dominated by debris flow [6, 19–23]. The hyperpycnal flow is recently attracting significant research attention. Zavala et al. explored the formation conditions, the dynamic characteristics, the sedimentary processes, and sedimentary principles of hyperpycnal flow and established a deposition model for the flow ([24, 25], 2011; [26–30]). In addition, the new technology of formation physical simulation research and engineering stress technology has provided technical support for the effective and economic development of tight oil and gas reservoirs [31–36].

The study of deep-water sediments in the Ordos Basin began in the 1970s, and divergent views exist on the large scale development of sandstones attributed to deep-water gravity flows in the basin. Chen et al. concluded that the deep-water sandstones of the Chang 6 and Chang 7 intervals are primarily turbidite deposits including slope displacement turbidite fans and slumping turbidite fans [37–41]. Zou et al. reported expansively developed debris flow sand bodies in the Chang 6 and Chang 7 intervals in the center of the basin [42–46]. Recent studies indicate that turbidity flow and debris flow deposits exist in the Ordos Basin [47–52]. In addition, Yang et al. found a gravity flow-induced sandstone different from those of debris flow and slumping turbidite sediments of the Chang 6 and Chang 7 intervals in the southern part of the basin, which are considered as hyperpycnal flow sediments [53, 54].

The knowledge from deep-water sedimentary research effectively guides the exploration and development of the Chang 7 reservoir formation and remains significant for exploration in the Ordos Basin. The Changqing Oilfield Company made a significant discovery in the Xin'anbian area of the central and western part of the basin in 2014. This represents the first tight field in China with over 100 million tons of proven reserves and highlights the significant exploration potential of the Chang 7 interval [55–57]. However, when compared with the central and western parts of the basin, no major discovery exists from exploration for tight oil in the southeast, with only occasional tight oil-enriched areas such as the Zhidan and the Ganquan. Detailed studies on the genetic types and sedimentary models of sand bodies in the Chang 7 interval in the southeast of the basin are scant. This study examines drilling core, logging, and analytical test data for more than 300 wells in the southeastern Ordos Basin and eight outcrop profiles (Shanshui River, Jinsuoguan, Yao Xian, Xuefengchuan, Hongshiya, Shiwang River, Yunyan River, and Yan River). The results reveal the characteristics, the sublacustrine fan development, and the significance of the gravity flow sediments for exploration in the Chang 7 interval in the southeastern Ordos Basin. The research results provide a theoretical basis for further exploration and development in the southeastern Ordos Basin.

2. Geological Setting

The Ordos Basin extends from the central to the western part of the North China Craton and is surrounded by the Helan-Liupan Mountain north-south tectonic belt to the west, the Pacific tectonic region in the east, and the Qilian-Qinling fold tectonic belt and the Tianshan-Xingmeng fold tectonic belt in the north and south, respectively (Figure 1). It is the second largest onshore sedimentary basin in China, with an area of about $37 \times 10^4\,km^2$ [58–63]. Under the influence of collision orogeny in Qinling area, the strata of the Middle and Late Triassic basin are generally high in the north and low in the south, thin in the north and thick in the south. The water body is characterized by a shallow north and a deep south, and the sedimentary range is much larger than that in the present basin. The Yanchang Formation consists of 1000–1300 m (3280–4265 ft) fluvial, delta, and lacustrine sediments [64, 65]. The evolution of the Yanchang Formation involves a period of early subsidence and extension (Chang 10-Chang 8 intervals), a peak stage (Chang 7 interval), and a late basin shrinkage stage (Chang 6-Chang 2 intervals) that continued and was followed by uplift and filling of the lake basin in the Late Triassic (Chang 1 interval) [64, 65]. Fluvial and lacustrine facies dominate the sediments, with thickness ranging from 1000 m to 1600 m [12, 49, 66–69] (Figure 2). The Chang 7 interval represents the peak stage of the Triassic lake development in the Ordos Basin. The basin experienced major subsidence during this period, affecting an area of over $5 \times 10^4\,km^2$, with water depth in the deep lake attaining 150 m (Figure 2). Deposition included dark mudstones and thick and abundant black shales named the "Zhangjiatan shale." These constitute the principal Mesozoic petroleum source rocks in the basin, with layer thickness of 15 m–30 m. Organic geochemistry data support the dark shale as the primary source rock for reservoirs in the basin because of the potential for hydrocarbon generation and expulsion associated with its high organic carbon content [70–75].

The study area lies in the southeast of the Ordos Basin bound in the south by Yan'an, in the north by Tongchuan, in the west by Yichuan, and in the east by Heshui and covers an area of about $4.4 \times 10^4\,km^2$. It belongs to the Yishan slope and partly to the northern margin of the Weibei uplift (Figure 1). The eight outcrops studied are mainly in the eastern and southern margins of the study area.

3. Data and Methods

This study is based on 240 wells' log data, 22 well cores, and several outcrops to interpret the gravity flows in the study area (Figure 1(b)). The outcropping sediments deposited during the Late Triassic, which were described in detail to illustrate the vertical characteristics of gravity flow deposits and interpret lithofacies. Then, the interval thickness and the ratio of sandstone thickness to interval thickness can be calculated through the integrated application of well logs, including gamma-ray, acoustic, and resistivity logging. Furthermore, casting thin section (CTS) observation and scanning electron microscopy (SEM) were used to analyze reservoir characteristics of sublacustrine fan sand bodies.

4. Results

4.1. Thickness Distribution. The average thickness of the Chang 7 interval in the study area ranges from 100 m to

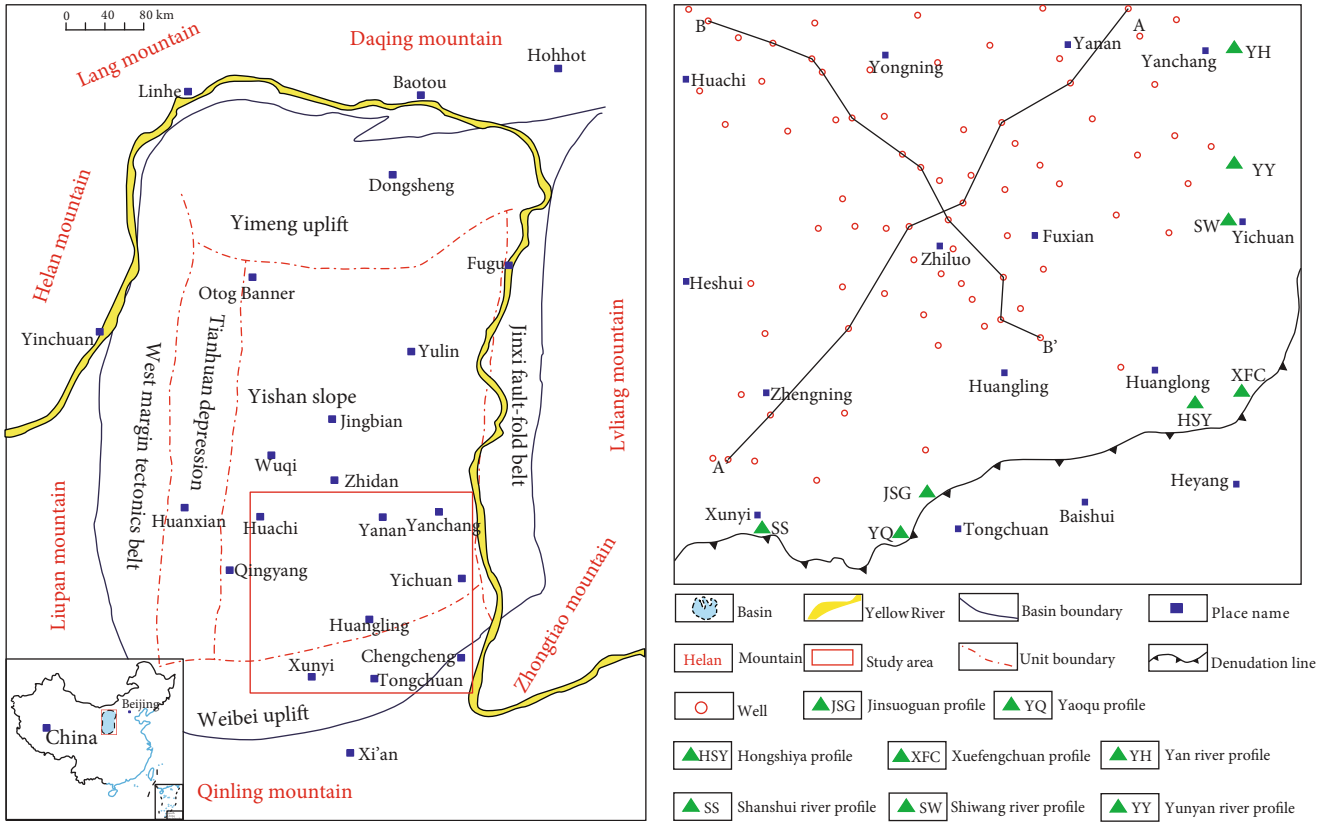

Figure 1: Location map of the Ordos Basin and the study area: (a) the structural units of the Ordos Basin and the study area location (modified from Yang et al.); (b) the area of study area with the included wells. The black line is the section depicted in Figure 10 with wells named.

160 m, with the maximum thickness in the middle of the study area. The maximum thickness is in the Zhiluo-Huangling area, with thicknesses of 140 m–160 m that indicating the center of the basin and the deepest part of the lake. The thickness of the strata decreases gradually to about 100 m–110 m in the west, north, and east. The area experienced subduction of the Yangtze Block to the North China Block in the Late Triassic and subduction of the Late Mesozoic Paleo-Pacific Plate to the North China Block. These caused uneven uplift in the basin, with erosion of strata of the Yanchang Formation in the southwest of the Yichuan-Huanglong-Binxian area (Figure 3).

4.2. Provenance Direction. We analyzed the characteristics of light minerals, heavy minerals, and detritus in outcrop sections and wells and divided the area into northeast, southern, and central portions, reflecting two provenance directions. The northeast and the southwest are indicated as the dominant provenance directions.

The heavy minerals in the Chang 7 reservoir strata mainly include zircon, garnet, leucosphenite, tourmaline, rutile, and subordinate amounts of chloritoid, epidote, and sphene [76–80]. The Fuxian-Yan'an area is the northeast provenance control area mainly comprises fine-grained lithic feldspar sandstones and feldspathic sandstones. The heavy minerals are the zircon–garnet assemblage, with generally over 50% garnet. The light minerals are dominated by feldspar containing over 50% and less than 30% quartz, suggesting low maturity sandstones. The Zhengning-Xunyi area is the south provenance control area, and its heavy minerals belong to the garnet–leucosphenite–zircon assemblage. The content of stable minerals such as zircon is generally over 40% and increases from the southwest to the center of the basin, whereas unstable minerals such as epidote decrease and are absent in some areas. The light minerals generally comprise 40%–50% quartz and about 20% feldspar, with an overall high compositional maturity. The zircon–tourmaline–rutile (ZTR) contour map displays increasing ZTR indices from the northeast, southwest, and south to the central region (Figure 4). Several heavy minerals occur in the central region, and the heavy mineral contents vary significantly. This indicates proximity to the sedimentary depocenter and is characteristic of a turbidity convergence zone affected by multiple provenances.

4.3. Sedimentary Characteristics

4.3.1. Turbidity Current Deposits. Turbidite deposits are widely distributed in the study area, and normal graded sequence is developed. Massive, parallel, horizontal, and cross-bedding can be observed in cores and field outcrops, showing incomplete Bouma sequence (Figures 5(a)–5(d)).

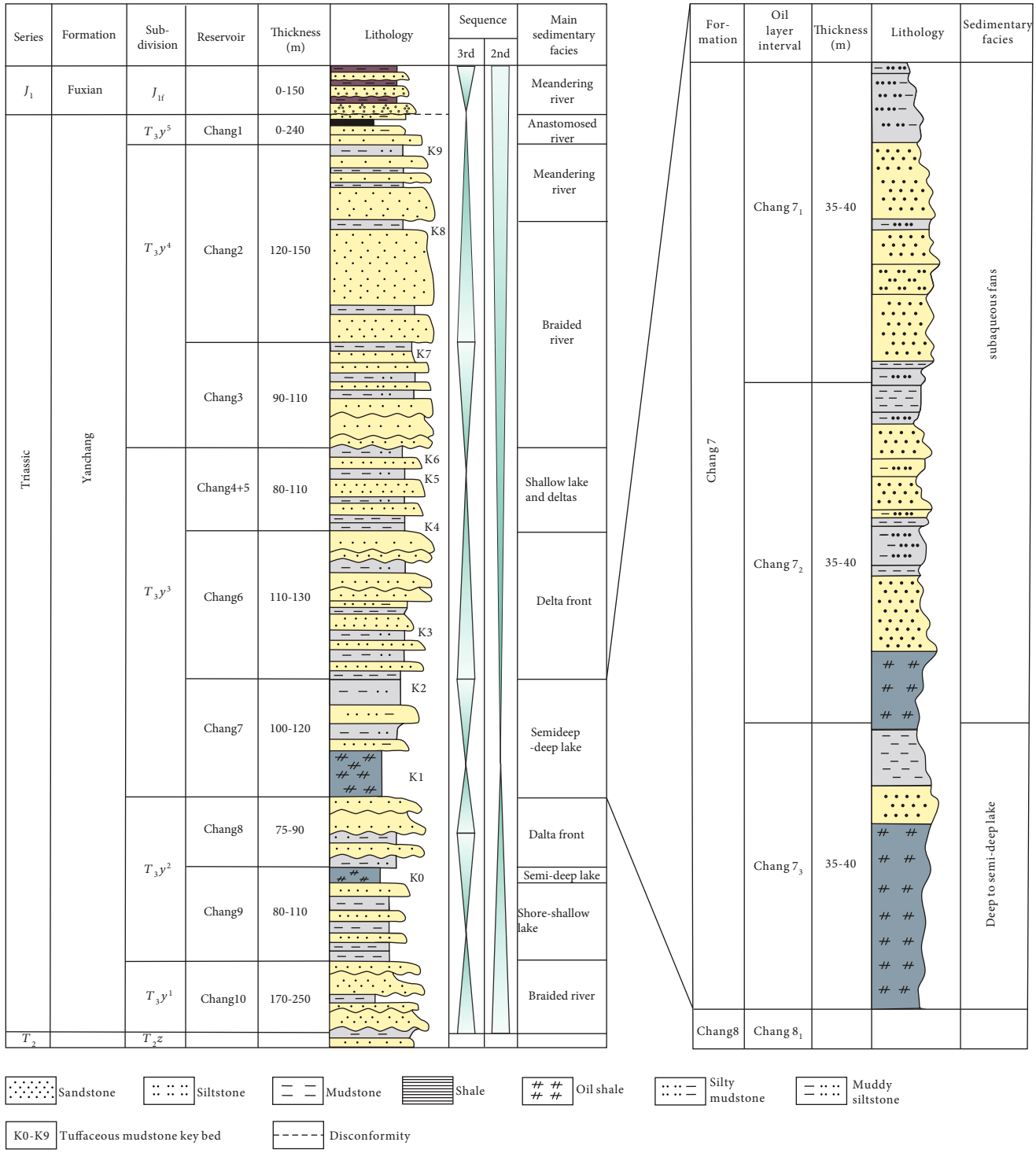

Figure 2: The generalized stratigraphic chart showing lithologies, sedimentary facies, the sequence stratigraphy, and evolution of the Yanchang Fm and Chang 7 interval in the Ordos Basin (the data were referenced from Yanhe outcrop and wells Z526 and Y221).

Incomplete Bouma sequences such as the ABC, the AB member, and other assemblages are mostly developed in sandstones (Figures 5(a)–5(d)). Flame structure, flute, and groove casts are developed at the bottom of turbidite sandstones (Figures 5(e)–5(i)). Muddy clastics are also common with abundant dark mudstone debris in the silty mudstones.

The grain size distribution curves for turbidity current deposits in the study area are characterized by straight line or approximate straight line (Figures 6(a) and 6(b)). The absence of rolling or saltation size populations, the high total suspended particle content, and the poor degree of sorting are typical particle size

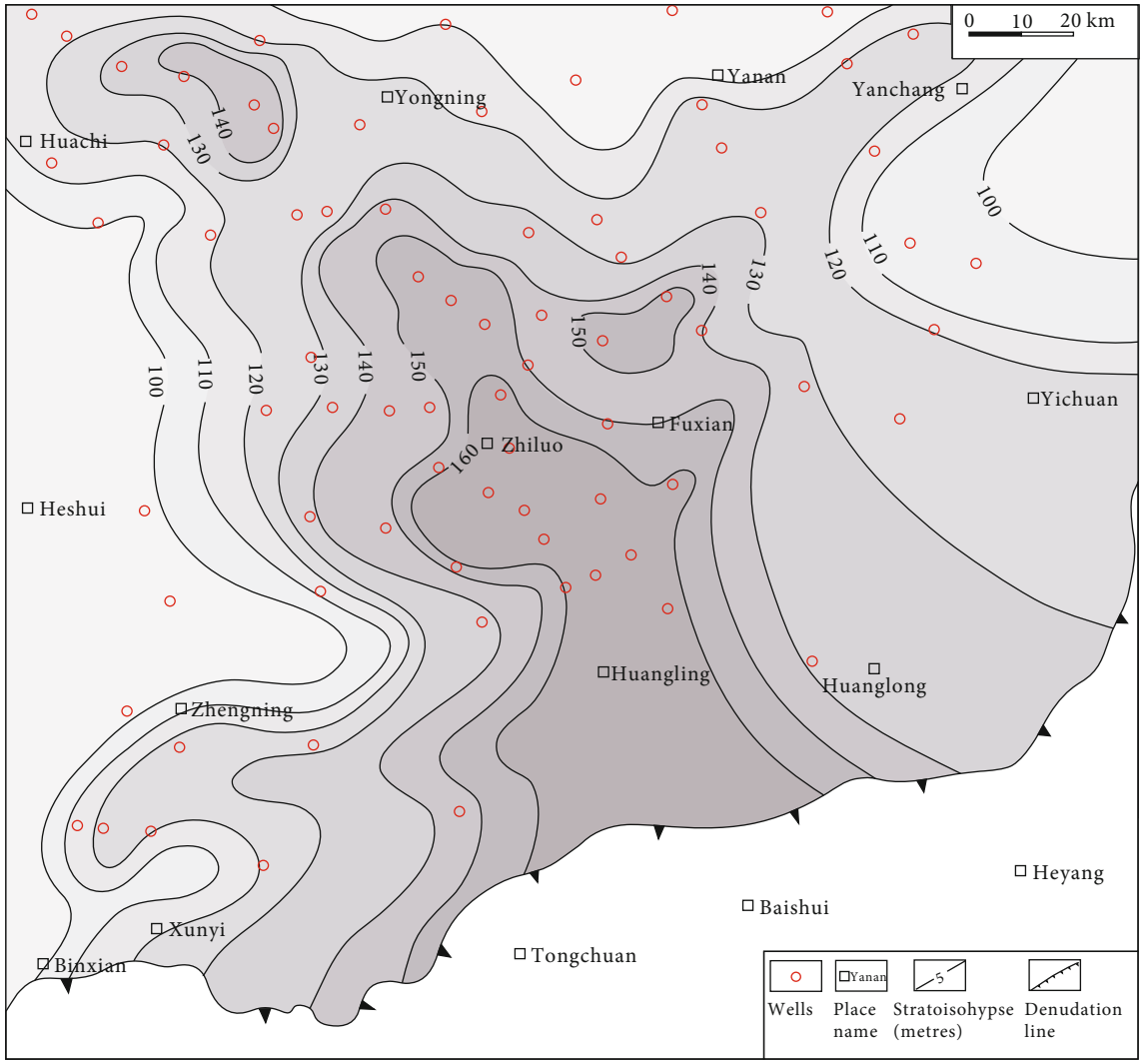

Figure 3: Strata thickness map of Chang 7 interval in southeast Ordos Basin.

characteristics of turbidites. The distribution of points parallel to the baseline on the C-M diagram (Figures 6(c) and 6(d)), which further supports deposition from turbidity currents.

4.3.2. Sand Debris Flow Deposits. Large-scale sandy debris flow deposits are developed in Chang7 interval of the study area. The typical lithology is massive fine sandstone associated with dark mudstone, siltstone, and fine sandstone rich in irregular mudstone (Figures 5(j)–5(o)). The thickness of single-layer sand body varies greatly, and the maximum thickness can be up to 5 m.

In the observation of core and field outcrop, the sandy debris flow deposit has the following characteristics: developed massive structure; some massive sandstone has a flushing surface at the bottom; and the massive sandstone is rich in irregular mudstone, and there are floating mudclasts at the top, which often show sharp contact with the overlying strata. The common sedimentary structures include flute and groove casts.

4.4. Well Log Characteristics. The characteristics of well logs are diagnostic of the sediments and sedimentary environments. Sedimentary facies and lithologies show peculiar and often distinct responses in well logs.

In this paper, the log facies characteristics of several sedimentary microfacies in the study area are presented on the basis of data including core descriptions and sedimentary structures (Table 1, Figure 7).

5. Discussions

5.1. Lithofacies Association and Facies Types. Field observations revealed the presence of Bouma sequences and that the longitudinal thickness of a layer of the sublacustrine fan sand body ranges from a few centimeters to a few meters in the study area. The horizontal distribution of the sand body is stable, and core observations confirm common thin mudstone and argillaceous siltstone intercalations of the sand body. The core characteristics and evolution from the sedimentary structures of the Chang 7 interval reveal subfacies

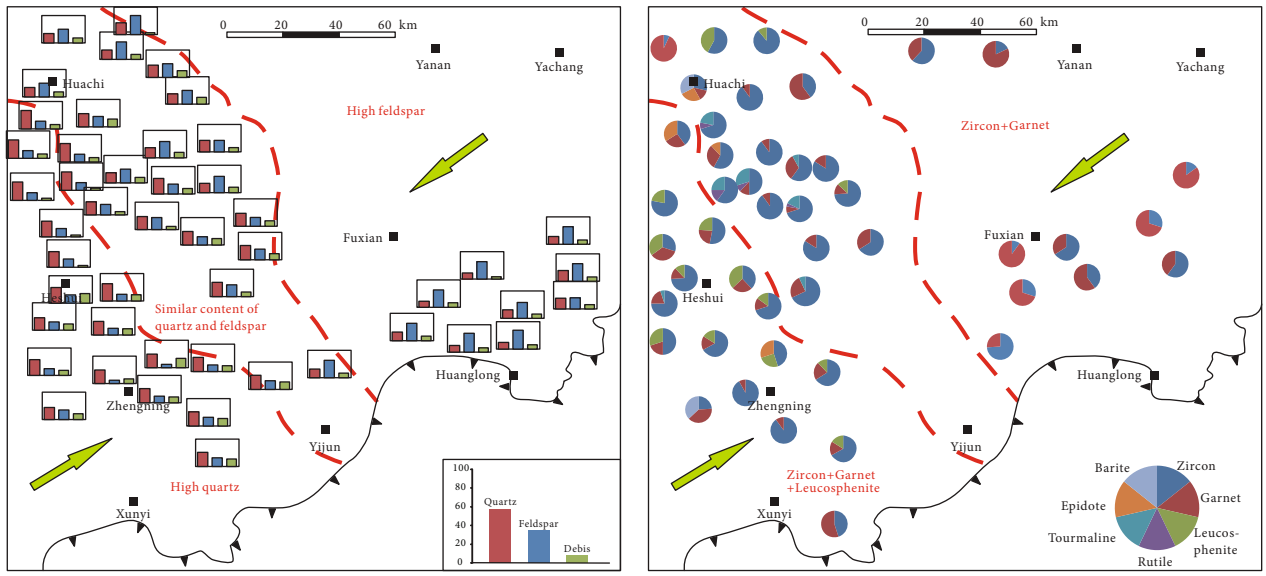

FIGURE 4: Light and heavy mineral distribution map in Chang 7 interval in the study area: (a) light minerals distribution; (b) heavy minerals distribution.

types including main channel, the branch channel, the interchannel, lobe fringe, and deep lake plain (Figure 7).

5.1.1. Main Channel Filling Deposits. The main channel filling deposits are close to the provenance area and includes the main channel and overflow deposits. The main channel filling deposits in the study area is not well developed than branch channel deposits. The main channel facilitated the transport of sediments along the slope characterized by the development of massive sandstones. The thickness of a sand body is over 1 m, whereas the thickness of a multistage superimposed sand body exceeds 10 m. The lithology is dominated by fine sandstones with graded bedding from bottom to top, with scour structures at the bottom. The Bouma sequence is characterized by repeated occurrence of the A or AB member. The planar distribution of the main channel reflects the topography, the flow direction, and the scale of the transported objects. The lateral thickness of the lenticular main channel sandstones changes rapidly, and the overflow deposits comprise mostly dark siltstones and mudstones (Figures 8(a) and 8(b)).

5.1.2. Branch Channel Filling Deposits. The branch channel filling deposits are generally developed in the middle and upper parts of sublacustrine fans, and the microfacies types include the branch channel and the interchannel. The branch channel is the extension of the main channel characterized by a weaker hydrodynamic condition. The sand body therefore is thinner, ranging from 0.3 m to 1 m, and the lithology is mainly fine sandstone. The branch channel microfacies represents the main facies of the sandstone reservoirs in the study area, with the Bouma sequence showing overlap of the AB and A members. The interchannel microfacies are mainly fine-grained sediments revealed by core observations to include irregular sand-shale interbeds, argillaceous siltstones, and silty mudstones, with a CDE Bouma sequence assemblage (Figures 8(b) and 8(c)).

5.1.3. Lobe Fringe and Deep Lake Plain. The terminal area of the sublacustrine fan deposition is mainly developed the lobe fringe. It intersects the deep lake plain and shows an inverse grading in the sections. Outcrop observations indicate the presence of dark shales, with a thin sandstone layer (<0.1 m thick) at the top (Figures 8(d)–8(g)).

5.2. Facies Distribution. Taking the Ch-72 period as an example, gravity-flow deposits developed widely in the deep lake, with sediments mainly accumulated in the northeast and south (Figures 9 and 10). The scale of sublacustrine fans increased as sublacustrine fans from different directions converged in the center of the study area, with sand bodies spreading smoothly.

The sand bodies of the sublacustrine fan in the northeast deep water area extend far, and six large fan bodies can be identified (Figures 9 and 10). The extension distance of the sublacustrine fan sand bodies in the southern deep water area is slightly shorter, and two large fans are developed (Figures 9 and 10). The main channel and branch channel were strip-shaped in plan, and the thickness of single sand bodies varies from 0.5 to 11 m, but composite sand bodies can reach more than 20 m. The channel sand bodies with single layer thickness more than 2 m are mostly caused by sandy debris flow, which can form reservoirs. The channel lateral margin sand bodies were strip-shaped, which are mostly a deposit combination of sandy debris flow, muddy debris flow, and turbidity current, with a thickness ranging from 0.2 m to 2.5 m. The lobe fringe was sheet-like in plan and developed multilayered

(a) (b) (c) (d) (e) (f) (g) (h)

Figure 5: Continued.

(i) (j)

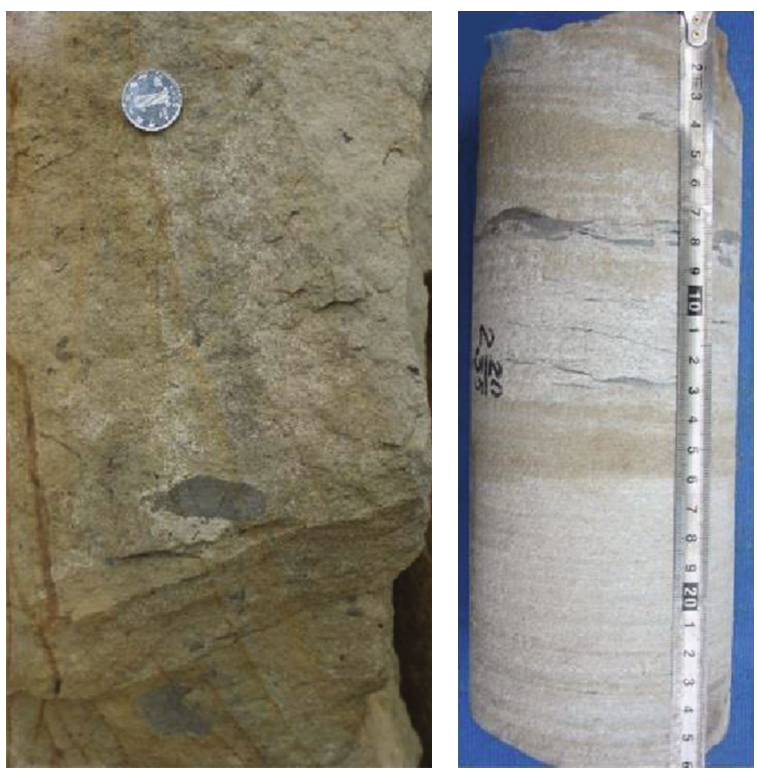

(k) (l)

Figure 5: Continued.

(m) (n)

(o)

Figure 5: Turbidity current deposits, and sand debris flow deposits characteristics of Chang 7 interval in the study area: (a) Bouma sequences, Hongshiya profile, Huanglong county; (b) Bouma sequences, Shiwang river profile, Yichuan county; (c) Bouma sequences, Shanshui river profile, Xunyi county; (d) Bouma sequences, Yaoqu profile, Yao county; (e) flute groove casts, Yaoqu profile, Yao county; (f) groove casts, Yaoqu profile, Yao county; (g) flute cast, well Z24, Chang 72; (h) flame structure, well H25, Chang71; (i) flame structure, well H25, Chang71; (j) irregular mudclasts, well X41, Chang 72; (k) floating mudclasts, Yaoqu profile, Yao county; (l) floating mudclasts, well ZT4, Chang7; (m) floating mudclasts and argillaceous parcel, well X99, Chang71; (n) sharp irregular contacts, well M9, Chang7; (o) sharp irregular contacts, well Y67, Chang7.

vertical mudstones. The thickness of single sand body ranges from 5 cm to 0.2 m, and the grain size is fine.

5.3. Depositional Models. The depositional model of the sublacustrine fan in the study area is established on the basis of data presented in this and previous studies (Figure 11). Contrary to a classical marine sublacustrine fan, the lacustrine fan of the study area does not develop large canyon channel in the study area. In addition, the boundary between the delta front sand bodies and the sublacustrine fan is not obvious.

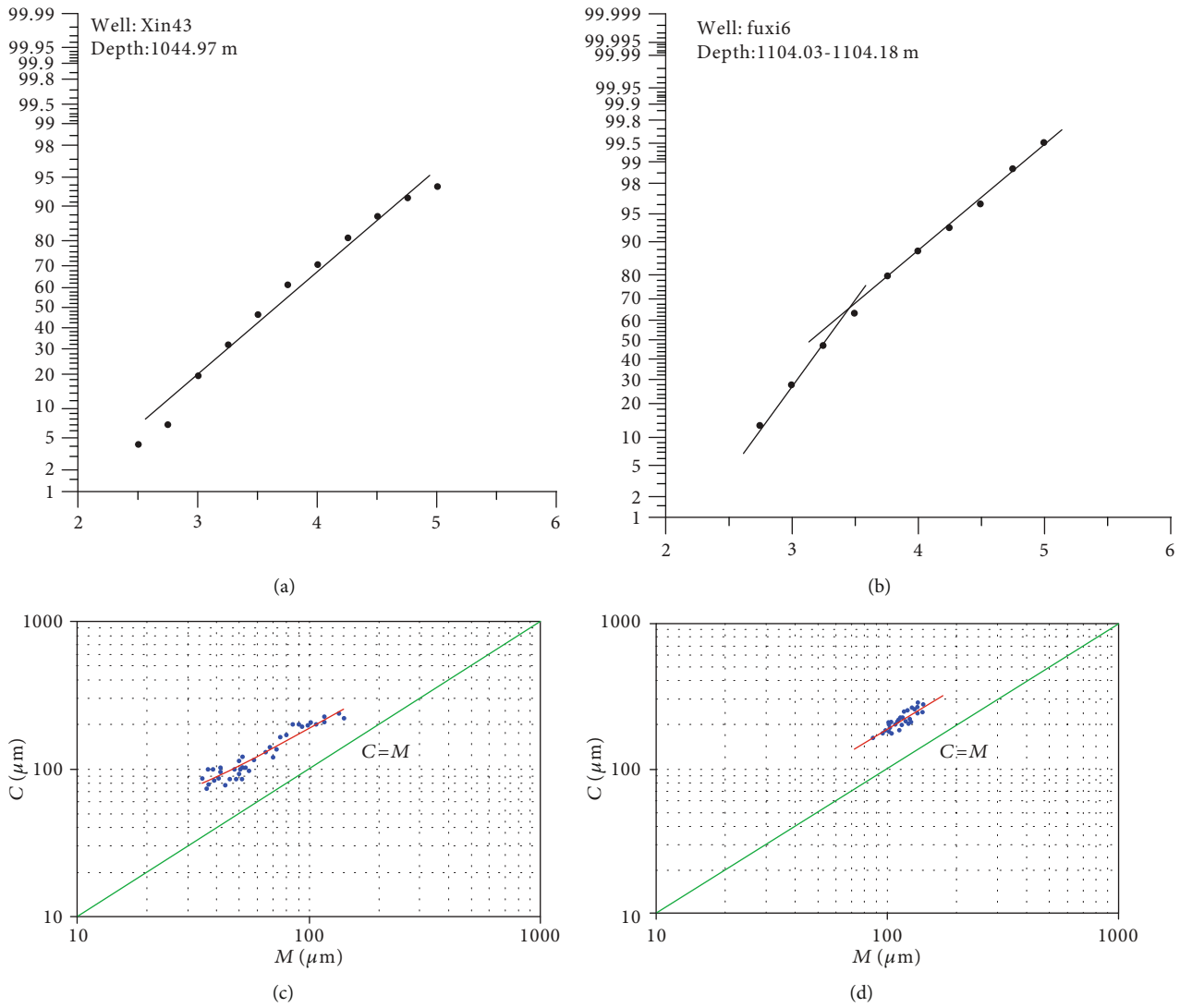

Figure 6: The grain size accumulation curve and C-M diagram in the study area: (a) the grain size accumulation curve, well X43; (b) the grain size accumulation curve, well FX6; (c) the C-M diagram, well X43; (d) the C-M diagram, well FX6.

The sublacustrine fan is lobed and tongue shaped in planar view, with a wide front at the fan margin and is lenticular in the longitudinal direction. The grain size of the fan sediments decreases away from the source.

Gravity flow deposits can be developed on both gentle and steep slopes of the lake basin, and the sedimentary types are controlled by both slope and provenance. In the northeast of the study area, the slope is gentle, and the provenance supply is sufficient. So the lacustrine fan developed in the deep water area is large, and most of the sand bodies are vertically superimposed along the provenance direction and extend to the center of the lake basin. On the other hand, the southern slope of the lake basin is steeper than that of the northeast, and the sublacustrine fan is also developed in the deep water area, but the scale is relatively limited, and the extension distance to the center of the lake basin is slightly shorter. The sublacustrine fan formed at the junction of the delta front and the slope belt. Factors such as earthquakes, volcanoes, and floods triggered stability loss of the sand body originally in the delta front, causing gravity flows including debris, turbidity, and grain flows. These flows transported large quantities of debris to deep portions of the lake area, with turbidity flow dominating during rapid transportation and terminating with the formation of sublacustrine fans in the relatively low-lying part of the lake basin. As the terrain slope becomes gentle, the main channel forks to form multiple branch channels, and the branch channels are easy to overlap with each other. After the branch channels enter the sublacustrine plain, with the further decrease of the terrain slope, the erosion of the gravity flow sediment to the underlying argillaceous sediment gradually weakens, and the channels disappear. In front of the channel, a wide lobed area is formed, and most of them are argillaceous siltstone and silty mudstone with thin sands.

Table 1: The characteristics of log facies of different sedimentary facies in the study area.

Facies	Microfacies	Characteristics GR logging curve characteristics	Geometry	Sedimentary structural	Lithology	Development position
Sublacustrine fan	Main channel		Box shape, zigzag box shape	Tabular cross bedding, trough cross bedding, massive bedding, graded bedding	Thick-bedded massive sandstone	Near the boundary of deep lake, the area where the sublacustrine fan has just entered the deep lake
	Overflow deposit		Zigzag box shape	Horizontal bedding, ripple cross bedding	Thin interbed of fine sand and mud	
	Branch channel		Zigzag box shape, bell-shaped shape	Tabular cross bedding, trough cross bedding, massive bedding, graded bedding	Medium to thin-bedded massive sandstone	
	Interchannel		Zigzag shape	Ripple cross bedding, horizontal bedding, deformed bedding	Thin interbed of fine sand and mud	

Table 1: Continued.

Facies	Microfacies	Characteristics GR logging curve characteristics	Geometry	Sedimentary structural	Lithology	Development position
	Lobefringe		Zigzag shape	Ripple cross bedding, horizontal bedding	Sheet-like turbidite sandstones and deep lake mudstones	The area adjacent to the deep lake plain at the outermost margin of the sublacustrine fan
Deep lake	Deep lake plain		Zigzag shape	Horizontal bedding, rich in siderite, deep lake fossils	Mudstone and shale	Deep lake center

5.4. Potential Implications in Hydrocarbon Exploration

5.4.1. Source Rock Distribution. The source rocks in the study area are mainly developed at the bottom of Chang 7 reservoir. The source rocks are distributed throughout the study area but generally lie along a NW-SW direction. The source rocks extend to Yanchang-Yichuan in the northeast, to Huachi in the northwest, to Zhengning-Xunyi in the southwest, and to Huangling-Huanglong in the southeast, with an effective distribution area of about $3.3 \times 10^4\ km^2$ (Figure 12). The thickness of the source rocks commonly exceeds 10 m, with a maximum thickness of 40–70 m. The source rock thickness generally decreases from the middle to the basin sides. The hydrocarbon generation center is in the area between Huachi and Huangling.

The principal reservoirs currently in the study area occur within or adjacent to Chang 7 source rocks. The close relationship between reservoirs and source rock distribution suggests a "source control."

5.4.2. Reservoir Characteristics of Sublacustrine Fan Sand Bodies

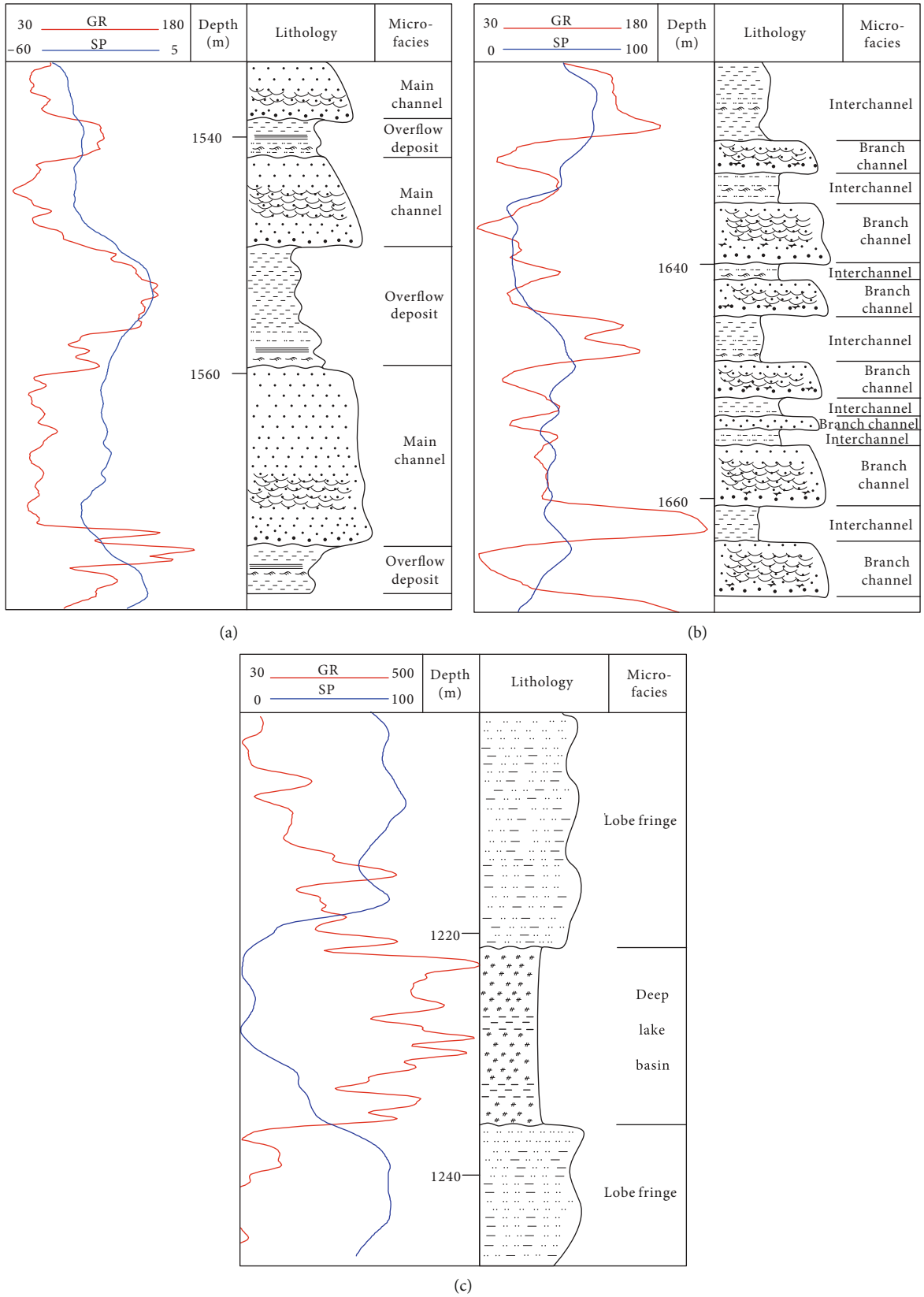

Figure 7: Characteristics of logging curves in different sedimentary facies: (a) logging curve characteristics of main channel filling deposits; (b) logging curve characteristics of branch channel filling deposits; (c) logging curve characteristics of lobe fringe.

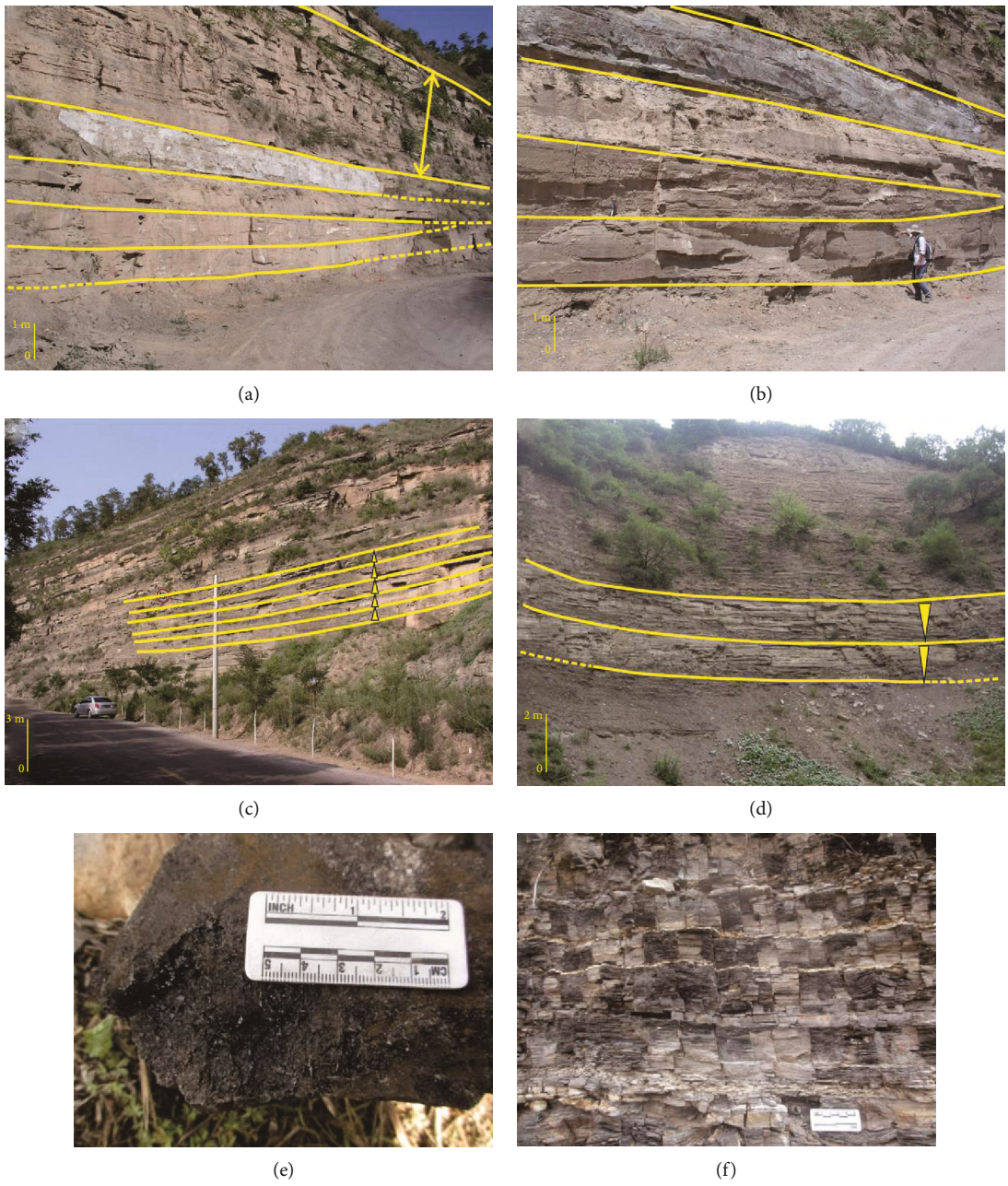

(a) (b) (c) (d) (e) (f)

Figure 8: Continued.

(g)

Figure 8: Outcrop of sublacustrine fan in southeastern Ordos Basin: (a) main channel deposits, Shanshui river profile, Xunyi county; (b) main channel deposits and branch channel deposits, Shanshui river profile, Xunyi county; (c) branch channel deposits and interchannel deposits, Shanshui river profile; (d) lobe fringe deposits, Niejiashan profile, Tongchuan city; (e–g) deep lake deposits, Tongchuan city.

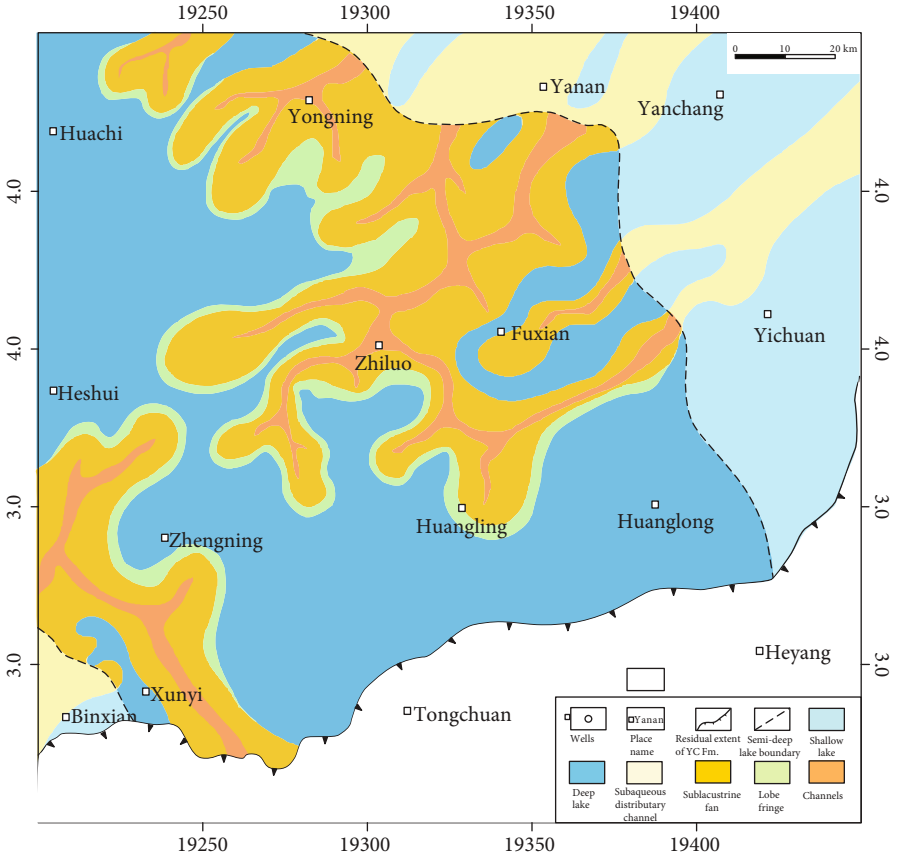

Figure 9: Sedimentary facies map of Chang 72 interval in the study area.

(1) Distribution of Sand Bodies in the Sublacustrine Fan. The extensive sublacustrine fan sand bodies accumulated in the semideep areas of the lake and constituted an important reservoir of the "tight oil near-source" accumulation. Turbidite sand bodies accumulated on a large scale in the Chang 7 interval of the study area, with reservoirs widely distributed from the delta front slope to the center of the basin. The sand bodies exhibit transverse and longitudinal superimposition in spatial distribution and constitute tight reservoirs. The sand bodies of the 1st layer of the Chang 7 reservoir are the most developed in the study area (Figure 13). The thickness of the sand body varies from 5 m to 25 m. From the 3rd layer to the 1st layer of the Chang 7 reservoir, the lake shoreline gradually decreased and allowed the sand body to advance toward the center of the deep lake, thereby increasing the extent of the sublacustrine fan. Concurrently, the multistage sand bodies were superimposed and continuously deposited. The wide distribution of sublacustrine fans and significant thickness of the sand bodies are suitable for the formation of tight reservoirs.

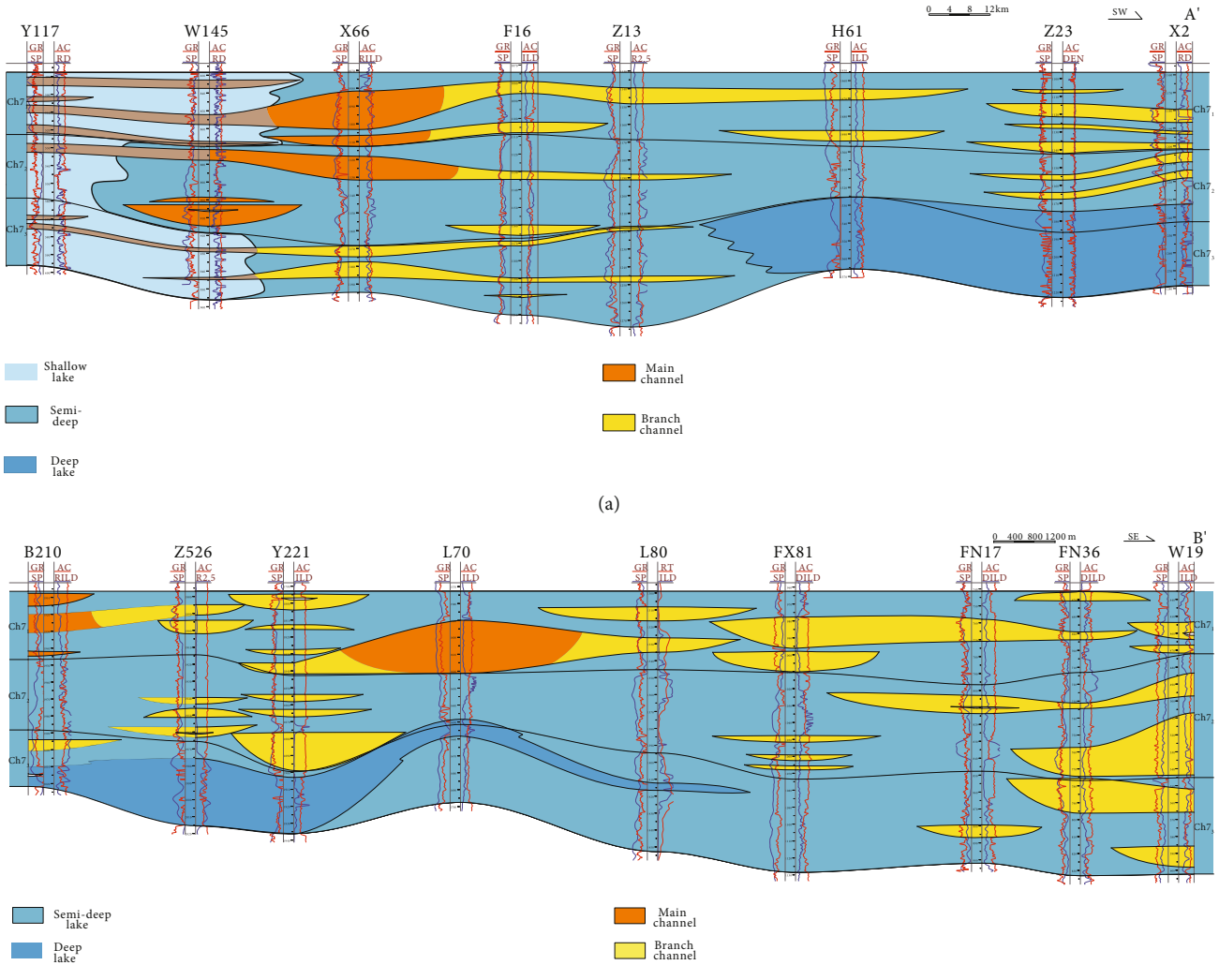

Figure 10: Cross section showing sedimentary facies distribution of Chang 7 interval in the study area (the section position is shown in Figure 1).

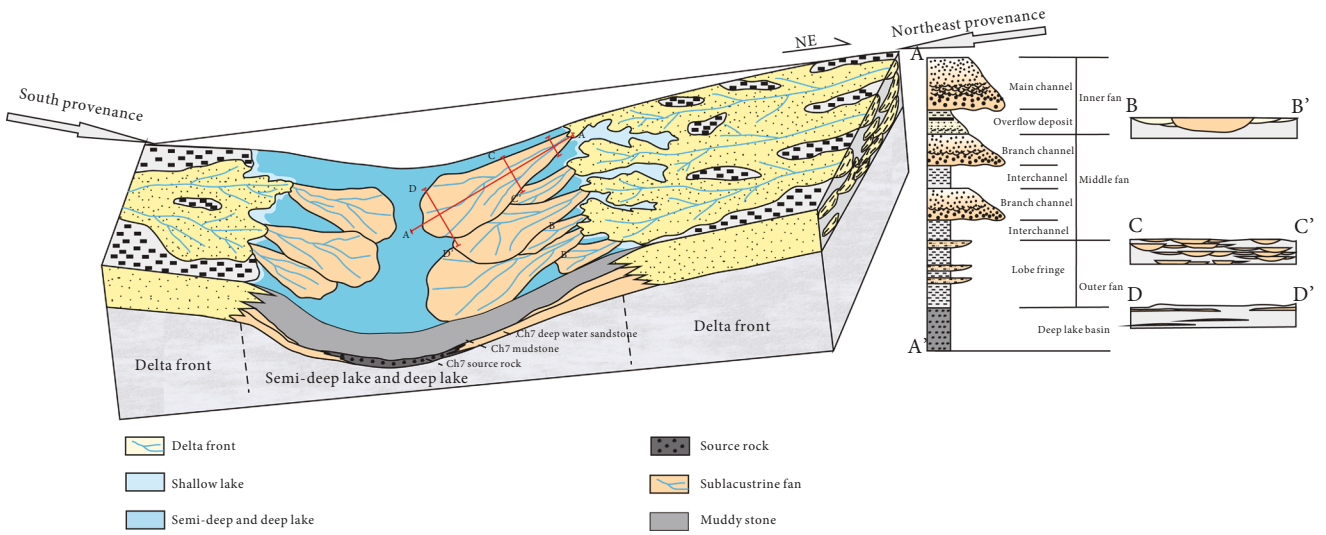

Figure 11: Depositional model of deep-water depositional systems in the Upper Triassic, southwestern Ordos Basin, and vertical sequence of all the three sedimentary microfacies.

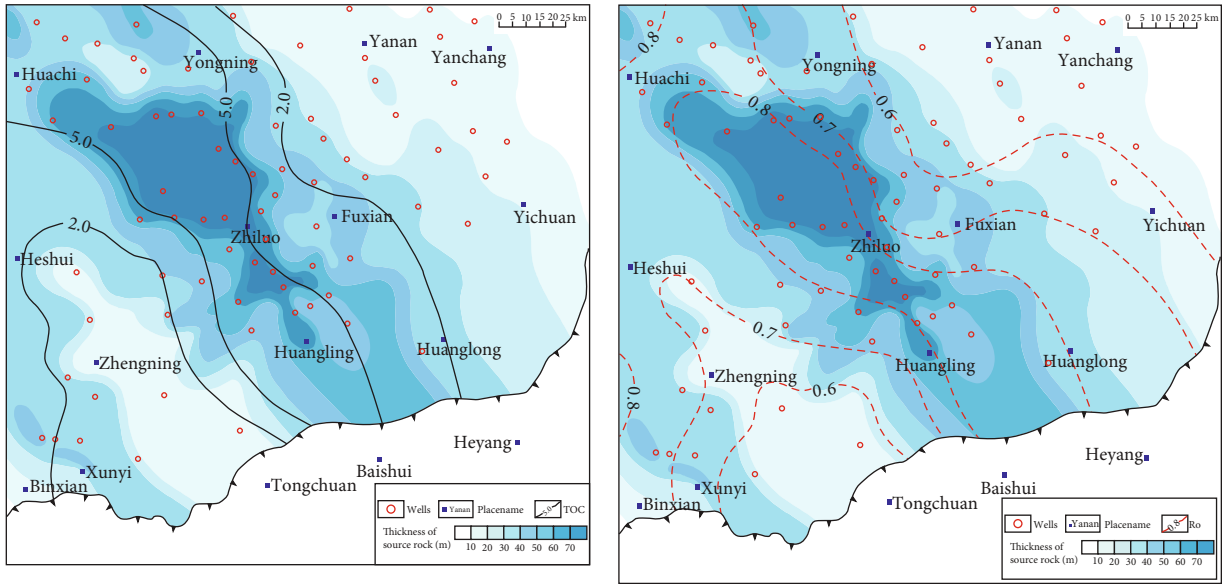

(a) (b)

Figure 12: Thickness of source rocks and contour line of R_o and TOC, Chang 7 interval, and southeastern Ordos Basin.

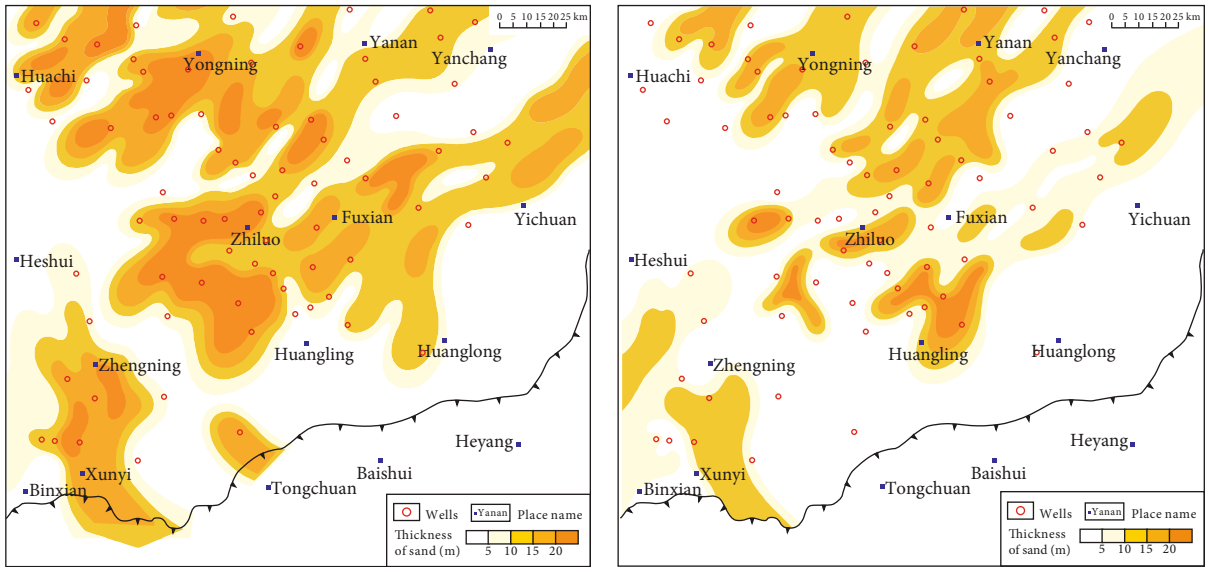

(a) (b)

Figure 13: Thickness of sand body in the study area: (a) thickness of sand body, Chang 7_1 oil layer; (b) thickness of sand body, Chang 7_2 oil layer.

(2) Pore Structure and Petrophysical Properties of Sublacustrine Fan Sand Bodies. The reservoir rock types are feldspathic sandstone and lithic feldspar sandstone, with moderate sorting and subangular grains. The main reservoir spaces of the Chang 7 reservoirs are primary intergranular pores, dissolved intergranular pores, dissolved intragranular pores, micropores, and microfracture pores (Figure 14), which are effective transport avenues for tight reservoirs.

The measured porosity varies from 6% to 8%, with an average value of 6.83%, and the permeability ranges from 0.1×10^{-3} to 0.5×10^{-3} μm^2, with an average value of 0.24×10^{-3} μm^2 (Figure 15). The reservoirs of the Chang 7 interval are tight, with the main channel and branch channel sandstones showing good petrophysical properties primarily hosting the tight reservoir oils.

5.4.3. Effective Source–Reservoir Relationship as an Important Factor for Accumulation. The horizontal and vertical distribution of turbidite sand bodies and source rocks partially controls the distribution of reservoirs. In the process of hydrocarbon generation, pressure build-up, and

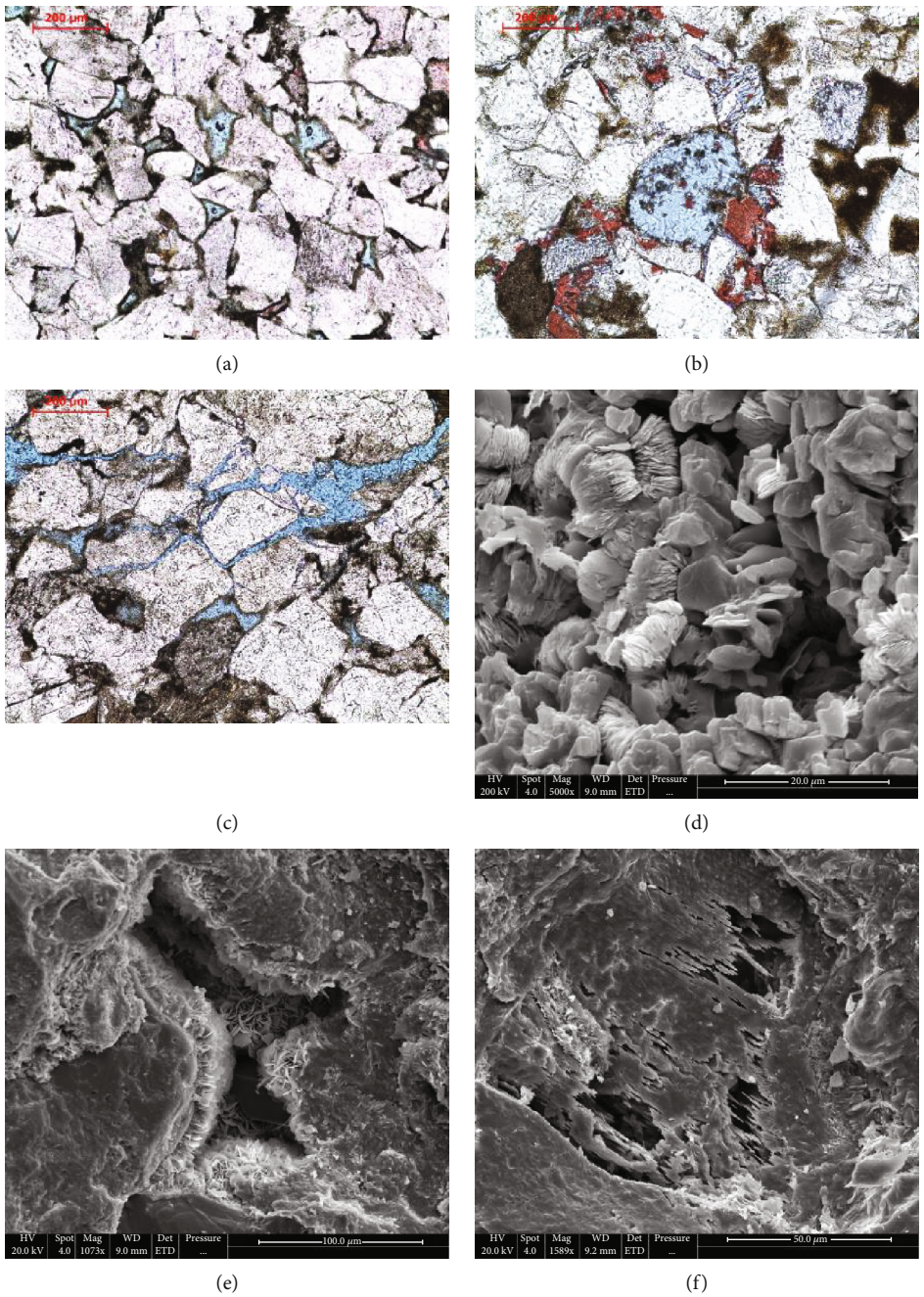

Figure 14: Pore types in the study area: (a) primary intergranular pores and dissolved intergranular pores, well X66, (-); (b) lithic dissolved pores, Shiwang river profile, (-); (c) microfracture pores, well X66; (d) intercrystalline pores, well X54, (-); (e) dissolved intergranular pores and grain-coating chlorite, Shiwang river profile; (f) feldspar dissolution pores, Shiwang river profile.

hydrocarbon expulsion, the generated oil first migrates to the adjacent horizons. The sublacustrine fan sand bodies extended to the basin center and established direct contact with the source rocks. The expelled oil accumulated in the reservoirs following short distance migration (Figure 16). The vertical superimposition of the thick sand bodies deposited by the main and branch channels formed large scale reservoirs and provided favorable conditions for oil accumulation. The dark mudstones in the Chang 7 interval were suitable for cap rock.

The relationship between the source rocks and the tight sandstone reservoirs in the Chang 7 interval in the study area reveals three types of source–reservoir assemblages including (1) thick sand bodies with multiple source rocks assemblage, (2) source rocks overlain by multiple medium-thick sandstone assemblage, and (3) source rocks overlain by multiple thin sandstone assemblage. The first two assemblages are the most favorable source and reservoir combinations and represent favorable exploration areas for tight oil.

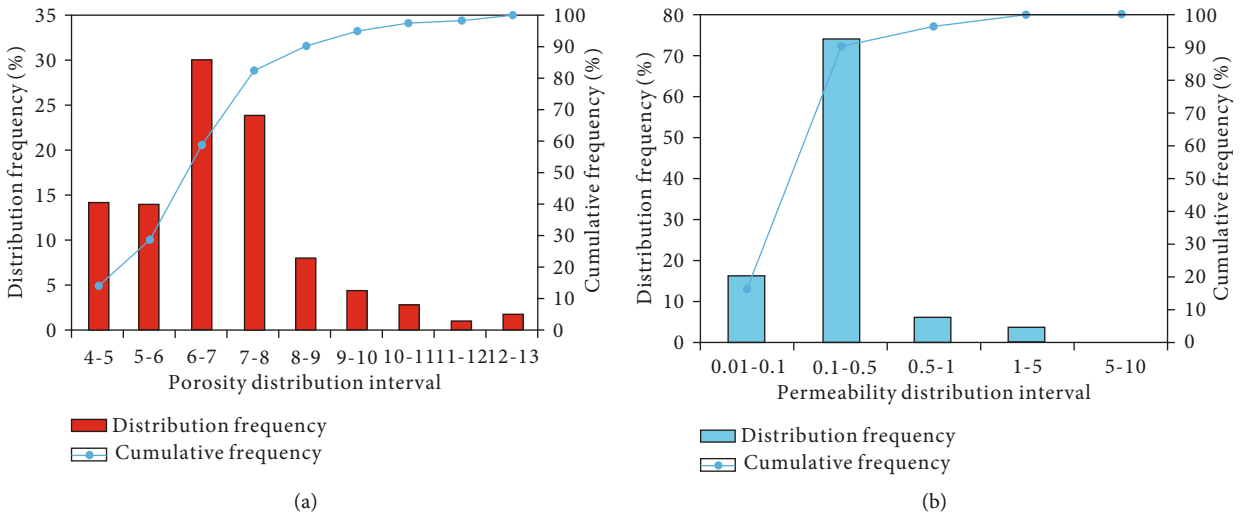

FIGURE 15: Porosity and permeability distribution frequency and cumulative frequency in the study area: (a) histogram of porosity distribution frequency; (b) histogram of permeability distribution frequency.

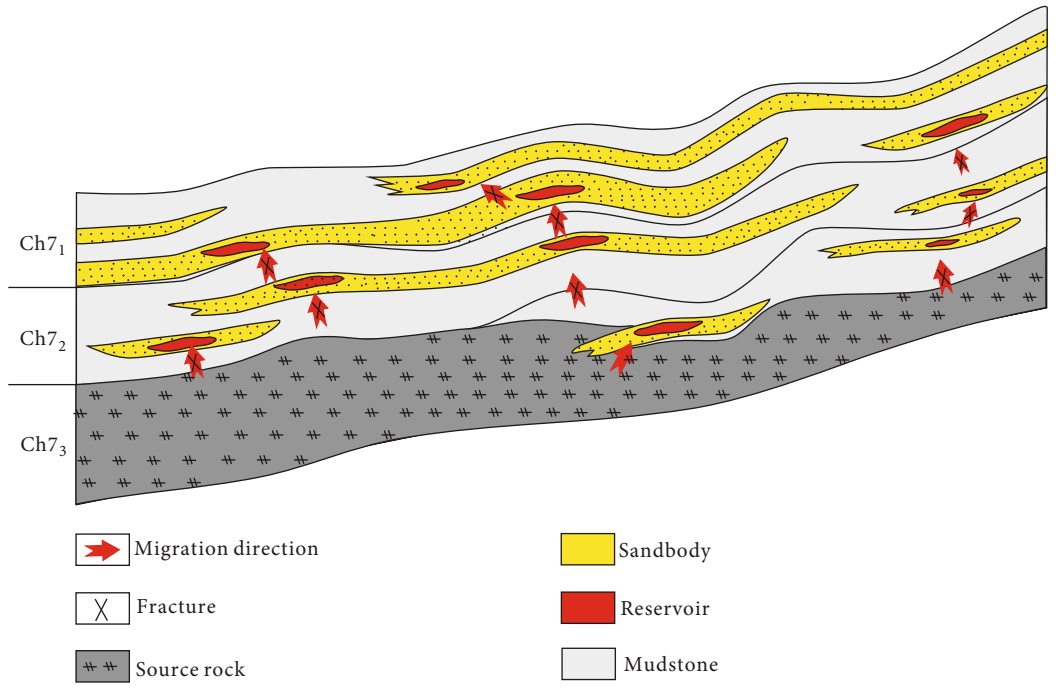

FIGURE 16: Reservoir forming model map of Chang 7 reservoir in southeast Ordos Basin.

6. Conclusions

(1) The main body of the Chang 7 interval of the Yanchang Formation in the southeastern Ordos Basin is a deep-water gravity flow system of semideep to deep lacustrine environment. The sublacustrine fan in the study area is a sublacustrine fan with gentle slope, without any erosion canyon between the sublacustrine fan sand bodies and delta front sand bodies. The sublacustrine fan is lobed and tongue shaped in planar view, with a wide front at the fan margin, and lenticular in the vertical direction. The grain sizes of the sublacustrine fan sediments decrease gradually away from the source

(2) Gravity flow deposits in the study area can categorised into three groups: sand debris flow deposits, turbidity current deposits, and deep-water mudstone deposits. The main channel and branch channel are mainly developed with thick massive sandy debris sandstone, while the channel lateral margin and branch channel lateral margin are mainly developed with middle massive sandy debris sandstones and

turbidite sandstones, which from bottom to top, the thickness of sand layer becomes thinner and the grain size becomes smaller

(3) The source rocks in the Chang 7 interval have generated and expelled sufficient oil for the formation of tight oil reservoirs. At the same time, the turbidite sand bodies of the Chang 7 interval overlying the source rock show properties suitable for tight reservoirs. The source–reservoir assemblages are capable of "self-generation, self-storage, and self-capping." The main and the branch channels are favorable exploration targets for tight oil and gas reservoirs

Abbreviations

Ch7: Chang 7 interval
CTS: Casting thin section
SEM: Scanning electron microscopy.

Data Availability

The data used in this manuscript available upon the author reasonable request.

Conflicts of Interest

The authors declare that they have no competing interests.

Acknowledgments

This work was supported by the National Key Research Project of China (No. 2016YFC0601003) and the National Natural Science Foundation of China (Grant Nos. 41172101, 51934005, and 52074226). We would like to appreciate the PetroChina Changqing Oilfield Company and Yanchang Oil Field CO., LTD for providing data collections.

References

[1] D. Duranti and A. Hurst, "Fluidization and injection in the deep-water sandstones of the Eocene Alba Formation (UK North Sea)," *Sedimentology*, vol. 51, no. 3, pp. 503–529, 2004.

[2] T. Meckel, "Classifying and characterizing sand-prone submarine mass-transport deposits," in *AAPG Annual Convention and Exhibition*, pp. 11–14, New Orleans, LA, 2010.

[3] K. Purvis, J. Kao, K. Flanagan, J. Henderson, and D. Duranti, "Complex reservoir geometries in a deep water clastic sequence, Gryphon Field, UKCS: injection structures, geological modelling and reservoir simulation," *Marine and Petroleum Geology*, vol. 19, no. 2, pp. 161–179, 2002.

[4] D. Z. Ren, F. Yang, R. X. Li, Y. H. Li, and D. K. Liu, "The influential factors and characteristics of tight sandstone gas reservoir: a case study in Ordos Basin in China," *Geofluids*, vol. 2020, 11 pages, 2020.

[5] G. Shanmugam, *Deep-Water Processes and Facies Models: Implications for Sandstone Petroleum Reservoirs*, Elsevier, 2006.

[6] G. Shanmugam, *New Perspectives on Deep-Water Sandstones: Origin, Recognition, Initiation, and Reservoir Quality*, Elsevier, 2012.

[7] G. Shanmugam, L. R. Lehtonen, T. Straume, S. Syvertsen, R. Hodgkinson, and M. Skibeli, "Slump and debris-flow dominated upper slope facies in the Cretaceous of the Norwegian and northern North Seas (61-67 N): implications for sand distribution," *AAPG Bulletin*, vol. 78, no. 6, pp. 910–937, 1994.

[8] G. Shanmugam, S. Shrivastava, and B. Das, "Sandy debrites and tidalites of Pliocene reservoir sands in upper-slope canyon environments, offshore Krishna-Godavari Basin (India): implications," *Journal of Sedimentary Research*, vol. 79, no. 9, pp. 736–756, 2009.

[9] A. Solheim, P. Bryn, H. Sejrup, J. Mienert, and K. Berg, "Ormen Lange–an integrated study for the safe development of a deep-water gas field within the Storegga Slide Complex, NE Atlantic continental margin; executive summary," *Marine and Petroleum Geology*, vol. 22, no. 1-2, pp. 1–9, 2005.

[10] C. H. Yang, X. Du, H. Pan, and T. Liu, "Advances in worldwide deep water hydrocarbon exploration and oil and gas exploration potential in the northern continental slope in South China Sea," *Earth Science Frontiers*, vol. 7, no. 3, pp. 247–256, 2000.

[11] G. Hu, W. Hu, J. Cao et al., "The distribution, hydrocarbon potential, and development of the Lower Cretaceous black shales in coastal southeastern China," *Journal of Palaeogeography*, vol. 6, no. 4, pp. 333–351, 2017.

[12] C. N. Zou, L. Wang, Y. Li, S. Tao, and L. Hou, "Deep-lacustrine transformation of sandy debrites into turbidites, Upper Triassic, Central China," *Sedimentary Geology*, vol. 265-266, pp. 143–155, 2012.

[13] A. H. Bouma, *Sedimentology of Some Flysch Deposits; a Graphic Approach to Facies Interpretation*, Published Ph. D (doctoral dissertation, thesis, Elsevier), 1962.

[14] E. Mutti, "Distinctive thin-bedded turbidite facies and related depositional environments in the Eocene Hecho Group (South-Central Pyrenees, Spain)," *Sedimentology*, vol. 24, no. 1, pp. 107–131, 1977.

[15] E. Mutti and F. R. Lucchi, "Turbidites of the northern Apennines: introduction to facies analysis," *International Geology Review*, vol. 20, no. 2, pp. 125–166, 2009.

[16] W. R. Normark, "Growth patterns of deep-sea fans," *AAPG Bulletin*, vol. 54, pp. 2170–2195, 1970.

[17] W. R. Normark, "Fan valleys, channels, and depositional lobes on modern submarine fans: characters for recognition of sandy turbidite environments," *AAPG Bulletin*, vol. 62, pp. 912–931, 1978.

[18] R. G. Walker, "Deep-water sandstone facies and ancient submarine fans: models for exploration for stratigraphic traps," *AAPG Bulletin*, vol. 62, no. 6, pp. 932–966, 1978.

[19] G. Shanmugam, "Ten turbidite myths," *Earth-Science Reviews*, vol. 58, no. 3-4, pp. 311–341, 2002.

[20] G. Shanmugam, "High-density turbidity currents; are they sandy debris flows?," *Journal of Sedimentary Research*, vol. 66, no. 1, pp. 2–10, 1996.

[21] G. Shanmugam, "50 years of the turbidite paradigm (1950s—1990s): deep-water processes and facies models—a critical perspective," *Marine and Petroleum Geology*, vol. 17, no. 2, pp. 285–342, 2000.

[22] G. Shanmugam, "Deep-marine tidal bottom currents and their reworked sands in modern and ancient submarine canyons," *Marine and Petroleum Geology*, vol. 20, no. 5, pp. 471–491, 2003.

[23] G. Shanmugam and R. Moiola, "Reinterpretation of depositional processes in a classic flysch sequence (Pennsylvanian

Jackfork Group), Ouachita Mountains, Arkansas and Oklahoma," *AAPG Bulletin*, vol. 79, no. 5, pp. 672–695, 1995.

[24] T. Mulder and J. P. M. Syvitski, "Turbidity currents generated at river mouths during exceptional discharges to the world oceans," *The Journal of Geology*, vol. 103, no. 3, pp. 285–299, 1995.

[25] T. Mulder, J. P. M. Syvitski, S. Migeon, J. Faugéres, and B. Savoye, "Marine hyperpycnal flows: initiation, behavior and related deposits. A review," *Marine and Petroleum Geology*, vol. 20, no. 6-8, pp. 861–882, 2003.

[26] T. Mulder and E. Chapron, "Flood deposits in continental and marine environments: character and significance," in *Sediment Transfer from Shelf to Deep Water-Revisiting the Delivery System*, R. M. Slatt and C. Zavala, Eds., pp. 1–30, American Association of Petroleum Geologists Studies in Geology, 2011.

[27] C. Zavala, M. Arcuri, and L. Valiente, "The importance of plant re-mains as diagnostic criteria for the recognition of ancient hyperpycnites," *Revue de Paléobiologie, Genève*, vol. 11, pp. 457–469, 2012.

[28] C. Zavala and M. Arcuri, "Intrabasinal and extrabasinal turbidites: origin and distinctive characteristics," *Sedimentary Geology*, vol. 337, pp. 36–54, 2016.

[29] C. Zavala, M. Arcuri, M. Di Meglio, and A. Zorzano, "Depósitos de turbiditas intra y extracuencales: origen y características distintivas," *IX Congreso de Exploración y Desarrollo de Hidrocarburos*, pp. 225–244, 2014.

[30] C. Zavala, M. Arcuri, H. Gamero, C. Contreras, and M. Di Meglio, "A genetic facies tract for the analysis of sustained hyperpycnal flow deposits," in *Sediment Transfer from Shelf to Deep Water-Revisiting the Delivery System*, R. M. Slatt and C. Zavala, Eds., vol. 61, pp. 31–51, American association of petroleum geologists, Studies in Geology, 2011.

[31] R. Jiang, F. Dai, Y. Liu, and A. Li, "Fast marching method for microseismic source location in cavern-containing rockmass: performance analysis and engineering application," *Engineering*, 2021.

[32] Q. X. Meng, W. Y. Xu, H. L. Wang, X. Y. Zhuang, W. C. Xie, and T. Rabczuk, "DigiSim – an open source software package for heterogeneous material modeling based on digital image processing," *Advances in Engineering Software*, vol. 148, p. 102836, 2020.

[33] Z. G. Tao, C. Zhu, M. C. He, and M. Karakus, "A physical modeling-based study on the control mechanisms of Negative Poisson's ratio anchor cable on the stratified toppling deformation of anti- inclined slopes," *International Journal of Rock Mechanics and Mining Sciences*, vol. 138, p. 104632, 2021.

[34] Z. G. Tao, C. Zhu, X. H. Zheng et al., "Failure mechanisms of soft rock roadways in steeply inclined layered rock formations," *Geomatics, Natural Hazards and Risk*, vol. 9, no. 1, pp. 1186–1206, 2018.

[35] Z. G. Tao, C. Zhu, X. H. Zheng, and M. C. He, "Slope stability evaluation and monitoring of Tonglushan ancient copper mine relics," *Advances in Mechanical Engineering*, vol. 10, no. 8, Article ID 168781401879170, 2018.

[36] Y. Wang, B. Zhang, S. H. Gao, and C. H. Li, "Investigation on the effect of freeze-thaw on fracture mode classification in marble subjected to multi-level cyclic loads," *Theoretical and Applied Fracture Mechanics*, vol. 111, p. 102847, 2021.

[37] Q. H. Chen, W. Li, Y. Gao et al., "The deep-lake deposit in the upper Triassic Yanchang Formation in Ordos Basin, China and its significance for oil-gas accumulation," *Science in China Series D: Earth Sciences*, vol. 50, no. S2, pp. 47–58, 2007.

[38] Q. H. Chen, W. Li, Y. Guo, J. Liang, J. Cui, and D. Zhang, "Turbidite systems and the significance of petroleum exploration of Yanchang Formation in the southern Ordos Basin," *Acta Geologica Sinica*, vol. 80, no. 5, pp. 656–663, 2006.

[39] Q. Fu, M. Lv, and Y. Liu, "Developmental characteristics of turbidite and its implication on petroleum geology in late-Triassic Ordos Basin," *Acta Sedimentologica Sinica*, vol. 26, no. 2, pp. 186–192, 2008.

[40] Q. S. Xia and J. Tian, "Sedimentary characteristics of sublacustrine fan of the interval 6 of Yanchang Formation of Upper Triassic in southwestern Ordos Basin," *Journal of Palaeogeography*, vol. 9, no. 1, pp. 33–43, 2007.

[41] J. X. Zhao, F. Li, X. Shen, Y. Luo, and W. Fu, "Sedimentary characteristics and development pattern of turbidity event of Chang 6 and Chang 7 oil reservoirs in the southern Ordos Basin," *Acta Petrolei Sinica*, vol. 29, no. 3, pp. 389–394, 2008.

[42] S. T. Fu, X. Deng, and J. Pang, "Characteristics and mechanism of thick sandbody of Yanchang Formation at the center of Ordos Basin," *Acta Sedimentologica Sinica*, vol. 28, no. 6, pp. 1081–1089, 2010.

[43] X. B. Li, H. Liu, S. Pan et al., "Subaqueous sandy mass-transport deposits in lacustrine facies of the Upper Triassic Yanchang Formation, Ordos Basin, Central China," *Marine and Petroleum Geology*, vol. 97, pp. 66–77, 2018.

[44] X. B. Li, H. Liu, Y. Wang, L. Wei, J. Liao, and Y. Ma, "First discovery of the sandy debris flow from the Triassic Yanchang Formation, Ordos Basin," *Lithologic Reservoirs*, vol. 21, no. 4, pp. 19–21, 2009.

[45] R. C. Yang, A. Fan, Z. Han, and A. J. Van Loon, "Lithofacies and origin of the Late Triassic muddy gravity-flow deposits in the Ordos Basin, central China," *Marine and Petroleum Geology*, vol. 85, pp. 194–219, 2017.

[46] C. N. Zou, Z. Zhao, H. Yang et al., "Genetic mechanism and distribution of sandy debris flows in terrestrial lacustrine basin," *Acta Sedimentologica Sinica*, vol. 27, no. 6, pp. 1065–1075, 2009.

[47] A. P. Fan, R. Yang, A. J. Van Loon, W. Yin, Z. Han, and C. Zavala, "Classification of gravity-flow deposits and their significance for unconventional petroleum exploration, with a case study from the Triassic Yanchang Formation (southern Ordos Basin, China)," *Journal of Asian Earth Sciences*, vol. 161, no. 1, pp. 57–73, 2018.

[48] J. J. Liao, X. Zhu, X. Deng, B. Sun, and X. Hui, "Sedimentary characteristics and model of gravity flow in Triassic Yanchang Formation of Longdong area in Ordos Basin," *Earth Science Frontiers*, vol. 20, no. 2, pp. 29–39, 2013.

[49] F. Liu, X. Zhu, Y. Li, M. Xue, and J. Sun, "Sedimentary facies analysis and depositional model of gravity-flow deposits of the Yanchang Formation, southwestern Ordos Basin, NW China," *Journal of the Geological Society of Australia*, vol. 63, no. 7, pp. 885–902, 2016.

[50] N. L. Sun, J. Zhong, S. Bao et al., "Sedimentary characteristics and petroleum geologic significance of deep-water gravity flow of the Triassic Yanchang Formation in southern Ordos Basin," *Journal of Palaeogeography*, vol. 19, no. 2, pp. 299–314, 2017.

[51] R. C. Yang, Z. He, G. Qiu, Z. Jin, D. Sun, and X. Jin, "Late Triassic gravity flow depositional systems in the southern Ordos Basin," *Petroleum Exploration and Development*, vol. 41, no. 6, pp. 661–670, 2014.

[52] R. C. Yang, Z. Jin, D. Sun, and A. Fan, "Discovery of hyperpycnal flow deposits in the Late Triassic lacustrine Ordos Basin," *Acta Sedimentologica Sinica*, vol. 33, no. 1, pp. 10–20, 2015.

[53] F. N. Sun, R. Yang, and D. Li, "Research progresses on hyperpycnal flow deposits," *Acta Sedimentologica Sinica*, vol. 34, no. 3, pp. 452–462, 2016.

[54] H. Yang, X. Niu, S. Luo, S. Feng, and Q. Lv, "Researh of simulatate experiment on gravity flow deposits of tight sand bodies of Chang 7 formation in Longdong area, Ordos Basin," *Earth Science Frontiers*, vol. 22, no. 3, pp. 322–332, 2015.

[55] J. H. Fu, S. X. Li, X. B. Niu, X. Q. Deng, and X. P. Zhou, "Geological characteristics and exploration of shale oil in Chang 7 Member of Triassic Yanchang Formation, Ordos Basin, NW China," *Petroleum Exploration and Development*, vol. 47, no. 5, pp. 870–883, 2020.

[56] H. J. Qu, R. Pu, J. Cao, Y. Zheng, W. Dong, and P. Guo, "Characteristics of Chang 7 tight oil reservoir in the southern Ordos Basin," *Unconventional oil and gas*, vol. 2, no. 1, pp. 1–9, 2015.

[57] J. L. Yao, X. Deng, Y. Zhao, T. Han, M. Chu, and J. Pang, "Characteristics of tight oil in Triassic Yanchang Formation, Ordos Basin," *Petroleum Exploration and Development*, vol. 40, no. 2, pp. 150–158, 2013.

[58] C. Y. Liu, H. Zhao, J. F. Zhao, J. Wang, D. Zhang, and M. Yang, "Temporo-spatial coordinates of evolution of the Ordos Basin and its mineralization responses," *Acta Geologica Sinica*, vol. 82, no. 6, pp. 1229–1243, 2008.

[59] X. M. Xiao, B. Zhao, Z. Thu, Z. Song, and R. W. T. Wilkins, "Upper Paleozoic petroleum system, Ordos Basin, China," *Marine and Petroleum Geology*, vol. 22, no. 8, pp. 945–963, 2005.

[60] B. Yang, H. Qu, R. Pu et al., "Controlling effects of tight reservoir micropore structures on seepage ability: a case study of the Upper Paleozoic of the Eastern Ordos Basin, China," *Acta Geologica Sinica*, vol. 2, pp. 322–336, 2020.

[61] R. C. Yang, Z. Jin, A. Van Loon, Z. Han, and A. Fan, "Climatic and tectonic controls of lacustrine hyperpycnite origination in the Late Triassic Ordos Basin, central China: implications for unconventional petroleum development," *AAPG Bulletin*, vol. 101, no. 1, pp. 95–117, 2017.

[62] Y. T. Yang, W. Li, and L. Ma, "Tectonic and stratigraphic controls of hydrocarbon systems in the Ordos basin: a multicycle cratonic basin in central China," *AAPG Bulletin*, vol. 89, no. 2, pp. 255–269, 2005.

[63] J. F. Zhao, N. P. Mountney, C. Liu, H. Qu, and J. Lin, "Outcrop architecture of a fluvio-lacustrine succession: upper Triassic Yanchang Formation, Ordos Basin, China," *Marine and Petroleum Geology*, vol. 68, pp. 394–413, 2015.

[64] C. N. Zou, X. Y. Zhang, P. Luo, L. Wang, Z. Luo, and L. H. Liu, "Shallow-lacustrine sand-rich deltaic depositional cycles and sequence stratigraphy of the Upper Triassic Yanchang Formation, Ordos Basin, China," *Basin Research*, vol. 22, no. 1, pp. 108–125, 2010.

[65] W. H. Li, X. Liu, Q. Zhang et al., "Deposition evolution of Middle-Late Triassic Yanchang Formation in Ordos Basin," *Journal of Northwest University (Natural Science Edition)*, vol. 49, no. 4, pp. 605–621, 2019.

[66] Y. Q. Liu, H. Kuang, N. Peng et al., "Mesozoic basins and associated palaeogeographic evolution in North China," *Journal of Palaeogeography*, vol. 4, no. 2, pp. 189–202, 2015.

[67] H. J. Qu, X. Yang, J. Cao, Y. Fan, and L. Guan, "Oil accumulation rules in deep zones of Upper Triassic Yangchang Formation in Ordos Basin," *Acta Petrolei sinica*, vol. 32, no. 2, pp. 243–243, 2011.

[68] K. L. Xi, Y. Cao, K. Liu et al., "Diagenesis of tight sandstone reservoirs in the Upper Triassic Yanchang Formation, southwestern Ordos Basin, China," *Marine and Petroleum Geology*, vol. 99, pp. 548–562, 2019.

[69] Q. H. Xu, W. Shi, X. Xie et al., "Deep-lacustrine sandy debrites and turbidites in the lower Triassic Yanchang Formation, southeast Ordos Basin, central China: Facies distribution and reservoir quality," *Marine and Petroleum Geology*, vol. 77, pp. 1095–1107, 2016.

[70] S. H. Lin, Z. Yang, L. Hou, X. Luo, and Q. Liu, "Geostatistic recognition of genetically distinct shale facies in Upper Triassic Chang 7 section, the Ordos Basin, North China," *Marine and Petroleum Geology*, vol. 102, pp. 176–186, 2019.

[71] C. Wang, Q. Wang, G. Chen et al., "Petrographic and geochemical characteristics of the lacustrine black shales from the Upper Triassic Yanchang Formation of the Ordos Basin, China: implications for the organic matter accumulation," *Marine and Petroleum Geology*, vol. 86, pp. 52–65, 2017.

[72] Z. J. Xu, L. Liu, T. Wang et al., "Characteristics and controlling factors of lacustrine tight oil reservoirs of the Triassic Yanchang Formation Chang 7 in the Ordos Basin, China," *Marine and Petroleum Geology*, vol. 82, pp. 265–296, 2017.

[73] H. Yang and W. Zhang, "Leading effect of the seventh member high-quality source rock of Yanchang Formation in Ordos Basin during the enrichment of low-penetrating oil-gas accumulation: geology and geochemistry," *Geochimica*, vol. 34, no. 2, pp. 149–154, 2005.

[74] H. Yang, X. Liang, X. Niu, S. Feng, and Y. You, "Geological conditions for continental tight oil formation and the main controlling factors for the enrichment: a case of Chang 7 member, Triassic Yanchang Formation, Ordos Basin, NW China," *Petroleum Exploration and Development*, vol. 44, no. 1, pp. 11–19, 2017.

[75] W. Z. Zhang, H. Yang, J. Li, and J. Ma, "Leading effect of high class source rock of Chang 7 in Ordos Basin on enrichment of low permeability oil gas accumulation," *Petroleum Exploration and Development*, vol. 33, no. 3, pp. 289–293, 2006.

[76] J. He, S. Feng, J. Huang, X. Yuan, P. Han, and Y. Li, "Effects of provenance on porosity development of Chang 6 sandstone of the Yanchang Formation in the center of Ordos Basin," *Acta Sedimentologica Sinica*, vol. 29, no. 1, pp. 80–87, 2011.

[77] J. He, S. Feng, X. Yuan, P. Han, G. Xie, and C. Zhang, "Sandstone compenent of outcrops of Yanchang Formation in the margin of Ordos Basin and its geological significance," *Lithologic Reservoirs*, vol. 23, no. 6, pp. 30–43, 2011.

[78] R. G. Wang, W. Li, Y. Liao, Y. Guo, and H. Liu, "Provenance analysis of Chang 7 member of Triassic Yanchang Formation in Ordos Basin," *Geological Bulletin of China*, vol. 32, no. 4, pp. 671–684, 2013.

[79] H. Yang, W. Dou, X. Liu, and C. Zhang, "Analysis on sedimentary facies of member 7 in Yanchang Formation of Triassic in Ordos Basin," *Acta Sedimentologica Sinica*, vol. 28, no. 2, pp. 254–263, 2010.

[80] C. L. Zhang, L. Zhang, T. Chen et al., "Provenance and parent-rock types of member 7 of Yanchang Formation (Triassic), Ordos Basin," *Acta Sedimentologica Sinica*, vol. 31, no. 3, pp. 430–439, 2013.